NASA Technical Memorandum 86345

NASA-TM-86345 19850007348

EFFECTS OF BODY SHAPE ON THE AERODYNAMICS OF A BODY OF REVOLUTION AT MACH NUMBERS FROM 1.6 TO 4.6

M. LEROY SPEARMAN

JANUARY 1985

National Aeronautics and
Space Administration

Langley Research Center
Hampton, Virginia 23665

SUMMARY

A wind-tunnel investigation has been made of the aerodynamic characteristics of several projectile-like bodies at Mach numbers from 1.6 to 4.63. The bodies had a length-to-diameter ratio of 6.67 and included three variations of forebody shape and four variations of afterbody shape. The results indicated that the lowest drag was achieved with a blunt forebody-cylinder at the lowest Mach number and with a cone-cylinder at the highest Mach number. The drag with the blunted forebody was essentially invariant with Mach number. The aerodynamic center location was the most rearward for the cone-cylinder and the most forward with the boattailed afterbody. With the exception of the boattailed afterbody, all of the bodies indicated inherent static stability above a Mach number of about 3 for a center-of-gravity location at about the 40-percent body station.

INTRODUCTION

The shape of a projectile may result from a number of considerations. These include the flight profiles desired, the speed and range necessary, volume requirements, launch considerations, guidance, propulsion, seeker, manufacturing techniques, cost, and so on. Many of the factors that might influence a projectile shape may also have an impact on the projectile aerodynamics. In turn, certain aerodynamic characteristics related to body shape may have an impact on the projectile performance and capability. It is the purpose of this paper to examine the effects of body shape on the aerodynamic characteristics of bodies of revolution representative of projectiles and to make some observations relative to shape changes on the projectile performance.

SYMBOLS

The coefficients used are normalized by the cylindrical cross-sectional area and body length, which were the same for all models. Nomenclature used is as follows:

a.c.	aerodynamic center
$C_{D,o}$	drag coefficient at $\alpha = 0°$
C_m	pitching moment coefficient, measured about nose
C_N	normal force coefficient
l	body length
M	Mach number
α	angle of attack, deg.

MODELS AND TESTS

The bodies of revolution investigated had a length-diameter ratio of 6.67 and are shown in figure 1. The models were a cone-cylinder, a circular-arc-cylinder, a blunt-nose-cylinder, a circular-arc-circular-arc, a circular-arc-cylinder-boattail, and a circular-arc-cylinder-flare. The forebody shape extended over the forward 45 percent of the body. The boattail and flare shapes were over the aft 10 percent of the body. The supersonic investigations extended over a Mach number range from 1.60 to 4.63 for angles of attack from minus 4 degrees to 60 degrees and include both force and pressure measurements as well as flow-visualization tests with Schlieren, vapor screen, and oil flow. A complete description of the models and the tests are contained in references 1 and 2 along with tabulated data and flow-visualization pictures. The present paper will be concerned with only a portion of the force data as related to the flight spectrum of projectiles. Base drag is included so that these results represent the unpowered flight of a projectile.

DISCUSSION

Typical Basic Data

Typical basic data extracted from reference 1 are shown in figures 2-4 for several bodies in the angle of attack range from 0 degrees to 8 degrees at M = 1.60 and 4.63. The circular-arc-cylinder and circular-arc-circular-arc are compared in figure 2. The results show greater load-carrying potential for the circular-arc-cylinder in the higher slope of C_N variations with angle of attack. In addition, a farther aft a.c. for the circular-arc-cylinder is indicated by the more negative slope of the variation of C_m with α.

The cone-cylinder and circular-arc-cylinder flare are compared in figure 3. These results indicate greater load-carrying potential for the flared body at both Mach numbers. The difference in flare effectiveness in providing stability is shown by the change from a less negative slope at M = 1.60 to a more negative slope at M = 4.63 in the variation of C_m with α.

The boattailed and the flared afterbody configurations are compared in figure 4. These results indicate the greater load-carrying potential for the flared body at both Mach numbers, as well as a more negative pitching moment variation with α.

Forebody Effect on Drag

The effects of forebody shape on the minimum drag with the cylindrical afterbody are shown in figure 5 as a function of Mach number. These effects were found to be somewhat dissimilar. At the lower Mach numbers (below about M = 3), the drag with the blunted forebody was lower than that for either the conical or the circular-arc forebodies with the difference becoming greater as the Mach number decreases. Such an effect has been noted in other instances (see reference 3) at transonic and low supersonic speeds. For such forebodies, having a fixed length and a fixed maximum diameter, the average surface slope is lower with the blunted nose and, as a result, the pressure drag behind the detached shock is lower. Above a Mach number of 3, the drag is lower for the conical forebody than for either the circular-arc forebody or the blunt forebody because of a lower energy loss through the forebody shock at these Mach numbers. It is interesting to note that the drag coefficient for the blunt forebody is nearly constant over the Mach number range from 1.60 to 4.63.

The minimum drag is compared in bar graph form for each test Mach number in figure 6. The lower drag for the blunt forebody is readily apparent at the lower Mach numbers, the near equalization of the drag at M = 2.96 is apparent, and the gradual emergence of the conical forebody as the lowest drag shape is apparent at the two higher Mach numbers.

Afterbody Effect on Drag

The effects of afterbody shape on the minimum drag with the circular-arc forebody are shown in figure 7 as a function of Mach number. These variations with Mach number do not show the type of dissimilarity that those noted for forebody changes. At Mach numbers below about 3, the drag is higher with either the flare or the boattail than with the cylinder and the circular-arc. The high drag for the flare at the lower Mach numbers is primarily a result of a shock produced by the flare and partly a result of a somewhat higher base drag. The high drag for the boattail is probably caused by separated flow over the afterbody that predominates in spite of a presumably smaller base drag. The increment in drag added by the boattail remains essentially constant over the Mach number range probably because the separated flow over the body remains. At Mach numbers above 3, the boattail afterbody results in the highest drag of the afterbody shapes investigated. The increment in drag due to the flare reduces progressively with increasing Mach number and, in fact, at the highest Mach number, the flared body appears to have slightly lower drag than any of the other afterbodies. This reduction occurs as the shock becomes attached to the flare at higher Mach numbers and the flare also probably serves to reduce the boundary layer growth over the length of the body.

A comparison of the afterbody drag effects is presented in bar-graph form in figure 8 for each test Mach number. At the two lower Mach numbers, the progressive increase in drag is apparent as the afterbody shape is varied from a cylinder, to a boattail, and to a flare. At the two higher Mach numbers, the emergence of the higher boattail drag appears and the progressive reduction for the flare can be seen. The drag level for the circular-arc afterbody, as indicated by a tick mark, is slightly lower than that for the cylinder at M = 1.60 and essentially the same as the cylinder at the other Mach numbers.

Effect of Forebody on Aerodynamic Center

The effects of the forebody shape on the aerodynamic center for the cylindrical afterbody are shown in figure 9 as a function of Mach number. Fairly large variations in a.c. occur between M = 1.6 and M = 3, but above M = 3, the a.c. location is almost invariant with Mach number as the transonic compressibility effects disappear. The variations are reasonably similar for the three shapes and, in general, indicate the most rearward location with the conical forebody and the most forward location with the circular-arc forebody. These locations of a.c. are apparently a result of the distribution of lift over the bodies with the conical forebody producing the least lift forward, thus resulting in a more rearward a.c. For each of these forebody shapes, an inherent static stability occurs for a c.g. of about 40-percent body length at Mach numbers above about 3. Such a c.g. location may not be difficult to achieve with a projectile. The effects of forebody shape on a.c. are shown in figure 10 for each Mach number in bar graph form. The more rearward location of a.c. for the conical nose at each Mach number is apparent.

Effect of Afterbody on Aerodynamic Center

The effects of afterbody shape on the aerodynamic center for the circular arc forebody are shown in figure 11. The transonic compressibility effects are again apparent at the lower Mach numbers. The variations with Mach number are reasonably similar with the most rearward location of a.c. occurring with the flare and the cylinder, and the most forward location occurring for the boattail and the circular arc. The considerably farther forward location of a.c. for the circular-arc-circular-arc body at the lower Mach numbers probably results from the fact that this body, having no discontinuities to produce shocks or promote separation, acts more like a subsonic airfoil and produces a peak pressure well forward on the body. The more rearward locations of a.c. for the flare and the cylinder probably occur because of the generation of more lift over the aft part of the body. Above a Mach number of about 3, static stability is inherent with the flare and the cylinder for a c.g. of about 40-percent body length. For the boattail and the circular-arc, however, a c.g. of about 30 to 35 percent would be required for inherent static stability. These effects of afterbody on the a.c. location are shown in bar-graph form in figure 12 for each Mach number. The more rearward location of a.c. for the flare and cylinder is readily apparent at each Mach number. The circular arc body, indicated by the tick mark, is shown to have a considerably more forward a.c. location at the lowest Mach number in comparison to the other bodies.

Minimum Drag for Various Bodies

The variations of minimum drag with Mach number for all bodies except the circular-arc-circular-arc, which is reasonably similar to the circular-arc-cylinder, are shown in figure 13. These results, which recap the results previously discussed for forebody and afterbody effects, show that, at the lowest Mach number, the drag is least with the blunt forebody and is the highest with the flared afterbody. At the highest Mach number, the drag is least with the conical forebody and the highest with the boattail afterbody. The most nearly constant variation of drag coefficient with Mach number occurred with the blunt forebody. Thus, in terms of minimum drag, the selection of the more optimum body shape is clearly dependent upon the Mach number requirements.

Aerodynamic Center for Various Bodies

The variations of a.c. location with Mach number are shown in figure 14 for all bodies except the circular-arc-circular-arc which is shown only at $M = 1.6$. At the higher Mach numbers, this body shows characteristics similar to the boattail afterbody. These results, which also recap results previously discussed for forebody and afterbody effects, show that the most rearward location of a.c. across the Mach number range occurs with the conical forebody. The most forward a.c. locations occurred with the circular-arc and the boattail afterbodies. Thus, in terms of inherent static stability trends, the best shape is the cone-cyclinder and the least desirable shapes are the circular-arc and boattailed afterbodies.

Normal Force for Various Bodies

The variations with Mach number of the normal-force coefficient for a constant angle of attack of 4 degrees are shown in figure 15 for various bodies. These results are indicative of the load-sustaining capability of the various body shapes when flying at angles of attack other than zero. Over the Mach number range, the flared body indicates the greatest ability to sustain a load with the circular-arc-cylinder

being the next best. While the ability of the other bodies to sustain a load are somewhat intertwined over the Mach number range, it appears that, in general, the blunt-nose body is the least capable.

Nonaerodynamic Considerations

Several aerodynamic features of body shape changes have been discussed. It should be recognized, however, that some nonaerodynamic factors may also enter into the selection of a projectile shape. While the scope of this paper could not possibly cover all other considerations pertinent to shape selection, some limited observations should be made:

- Manufacturing.- It is possible that, depending on the material used and the manufacturing technique employed, some shapes may be simpler and less costly to make than others.

- Seekers.- If a form of seeker is employed in a projectile, there are some nose shapes more amenable to the type of seeker used than other shapes might be.

- Volume.- In the total volume requirements or in the required internal distribution of volume, certain shapes may be more adaptable than others.

- Propulsion.- If any form of on-board propulsion is used, then certain shapes, particularly the afterbody, may be more suitable than others.

- Launch.- From a consideration of possible launch constraints and perhaps even storage requirements, some shapes may be less desirable than others.

CONCLUDING REMARKS

An investigation has been made of the aerodynamic characteristics of a series of bodies of revolution at Mach numbers from 1.60 to 4.63. Each of the six bodies investigated had a length-to-diameter ratio of 6.67. Modifications included three forebody shapes over the forward 45 percent of a body having a cylindrical afterbody, and three afterbody shapes for a body with a circular-arc forebody. Some concluding observations from the investigation are:

- The lowest drag was produced at the lowest Mach number with a blunt forebody-cylinder, and at the highest Mach number, with a cone-cylinder.

- The highest drag was produced at the lowest Mach number with a flared afterbody and, at the highest Mach number, with a boattailed afterbody.

- The drag with the blunted forebody was essentially invariant with Mach number.

- The farthest aft aerodynamic center locations were obtained with the cone-cylinder and the most forward locations with the boattailed afterbody.

- With the exception of the boattail afterbody, all body shapes indicated inherent static stability above a Mach number of about 3 with a center of gravity location of about 40-percent body length.

- While the aerodynamic effects investigated produced reasonably clear results, the shaping of a body should also take into consideration such other things as manufacturing, seekers, volume requirements, propulsion, launchers, storage, and so on.

REFERENCES

1. Landrum, Emma Jean; and Babb, C. Donald: Wind-Tunnel Force and Flow-Visualization Data at Mach Numbers From 1.6 to 4.63 for a Series of Bodies of Revolution at Angles of Attack From -4° to 60°. NASA TM-78813, 1979.

2. Landrum, Emma Jean: Wind-Tunnel Pressure Data at Mach Numbers From 1.6 to 4.63 for a Series of Bodies of Revolution at Angles of Attack From -4° to 60°. NASA TM X-3558, 1977.

3. Corlett, William A.; and Howell, Dorothy T.: Aerodynamic Characteristics at Mach 0.60 to 4.63 of Two Cruciform Missile Models, One Having Trapezoidal Wings With Canard Controls and the Other Having Delta Wings With Tail Controls. NASA TM X-2780, 1973.

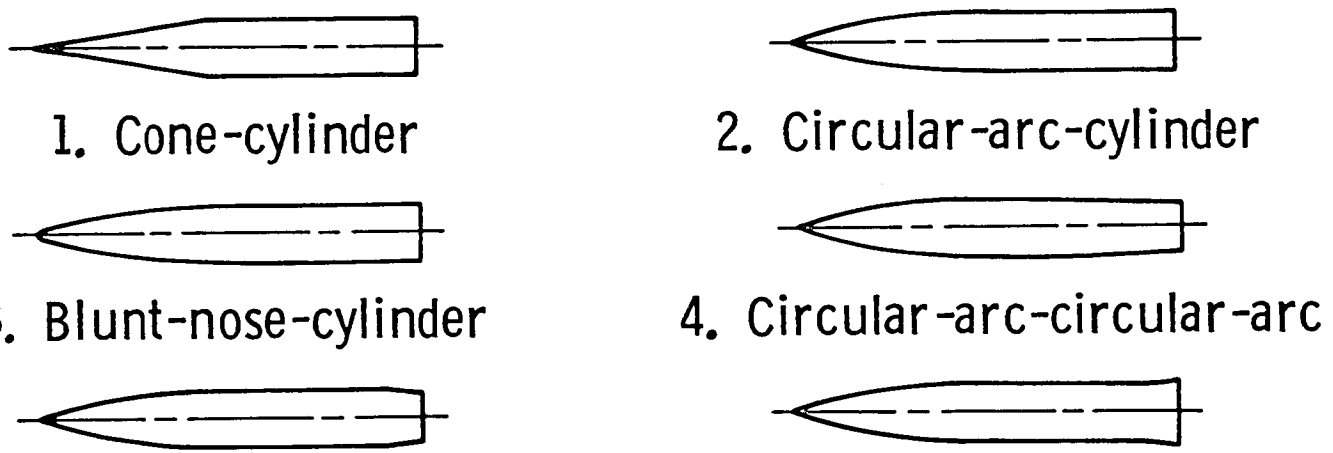

Figure 1.- Test bodies, l/d = 6.67.

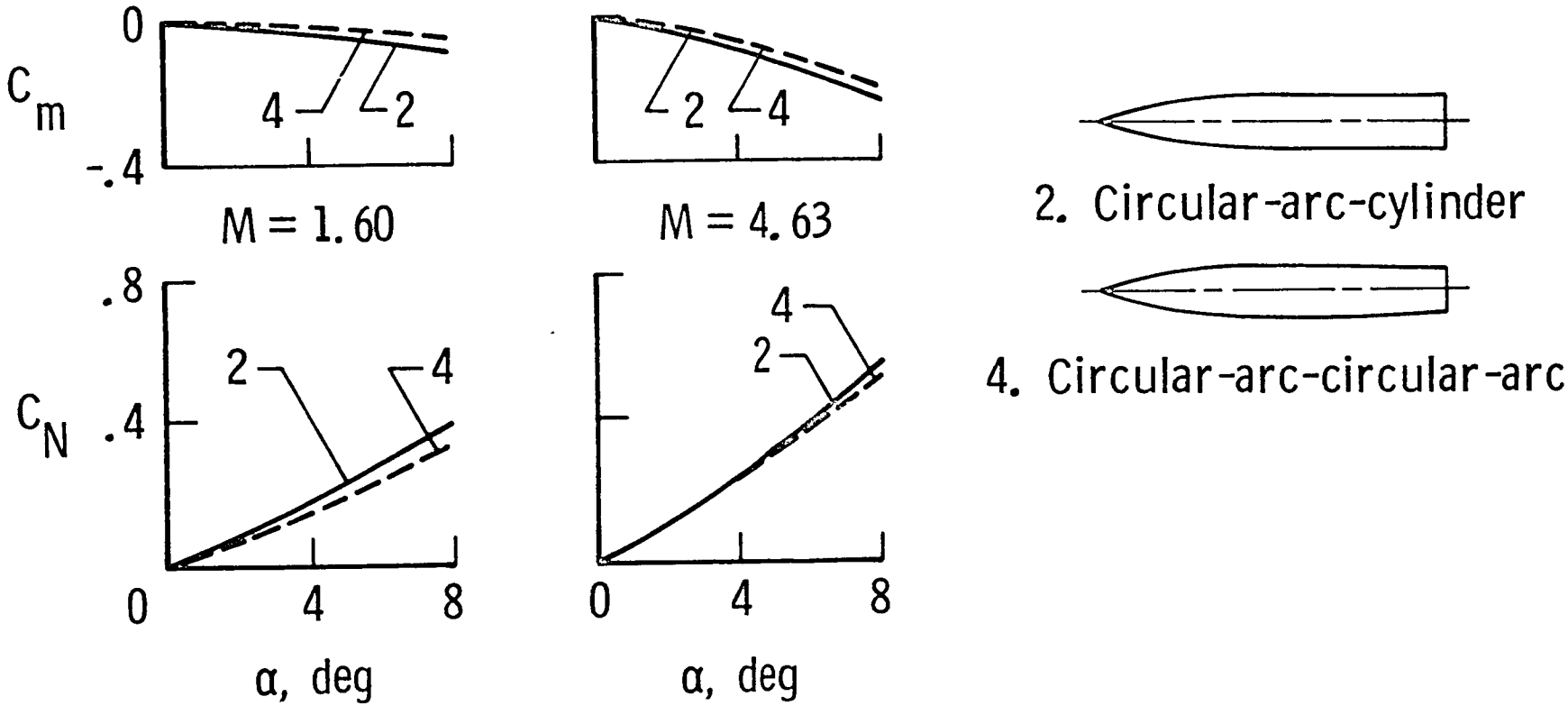

Figure 2.- Basic data for circular-arc-cylinder and circular-arc-circular-arc bodies at M = 1.60 and 4.63.

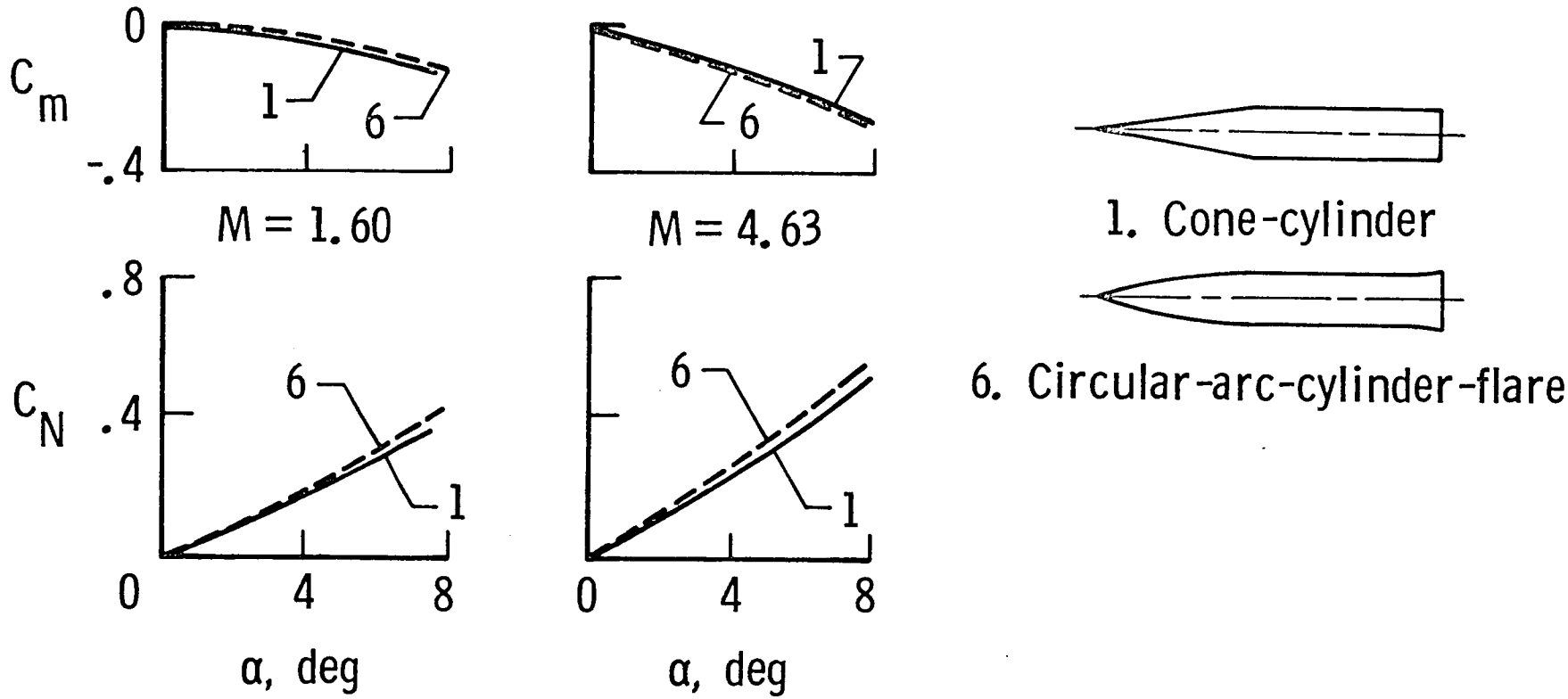

Figure 3.- Basic data for cone-cylinder and circular-arc-cylinder-flare bodies at M = 1.60 and 4.63.

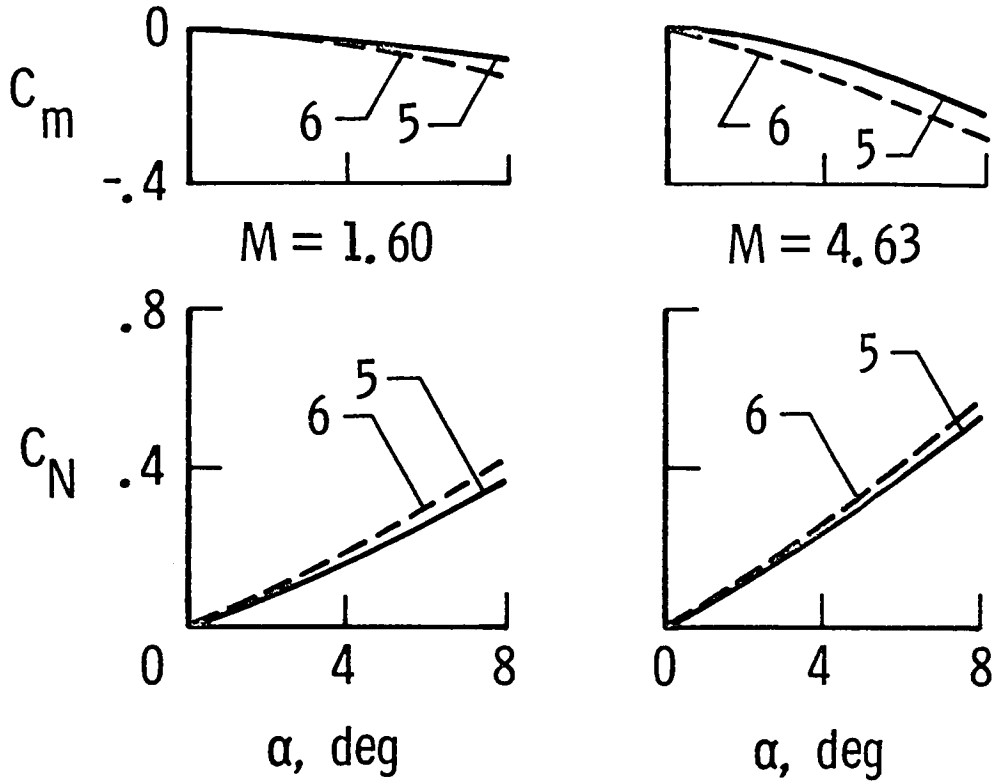

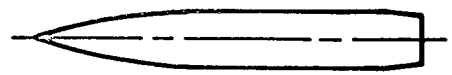

5. Circular-arc-cylinder-boattail

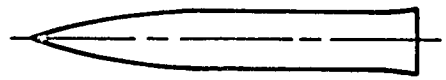

6. Circular-arc-cylinder-flare

Figure 4.- Basic data for circular-arc-cylinder-boattail and circular-arc-cylinder-flare bodies at M = 1.60 and 4.63.

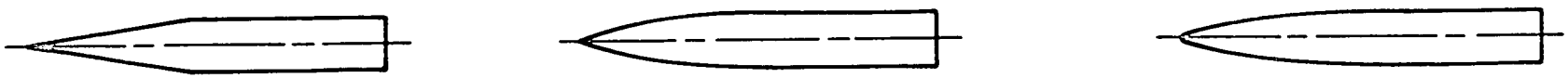

1. Cone-cylinder

2. Circular-arc-cylinder

3. Blunt-nose-cylinder

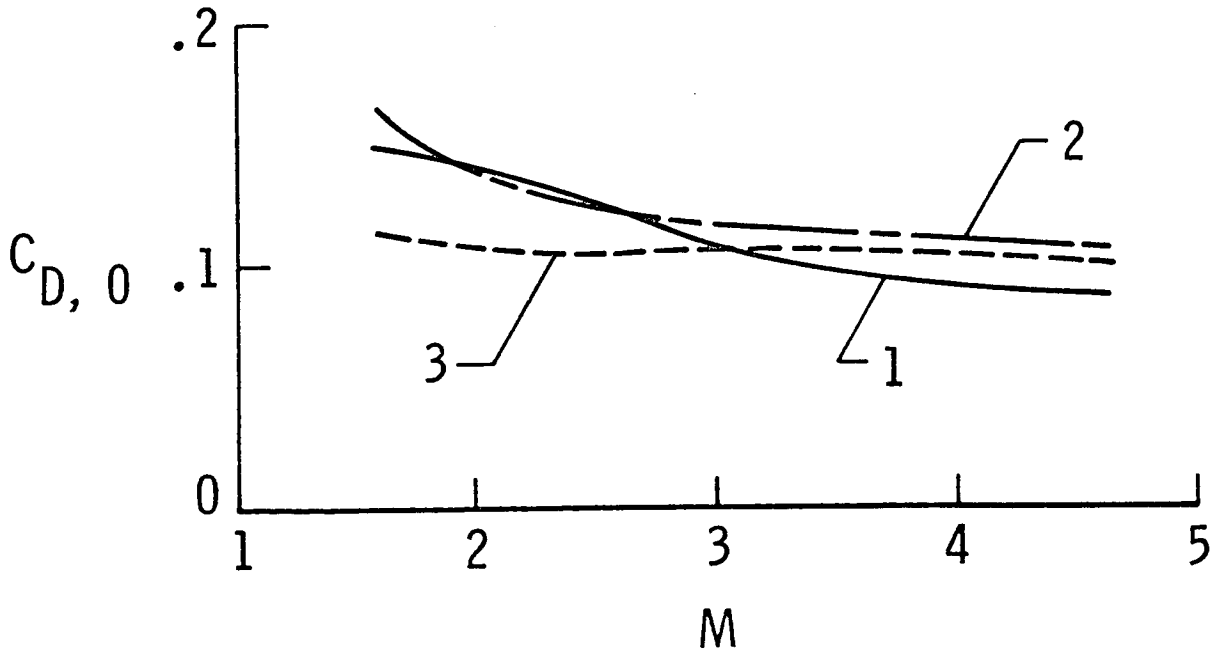

Figure 5.- Forebody effect on minimum drag with cylindrical afterbody.

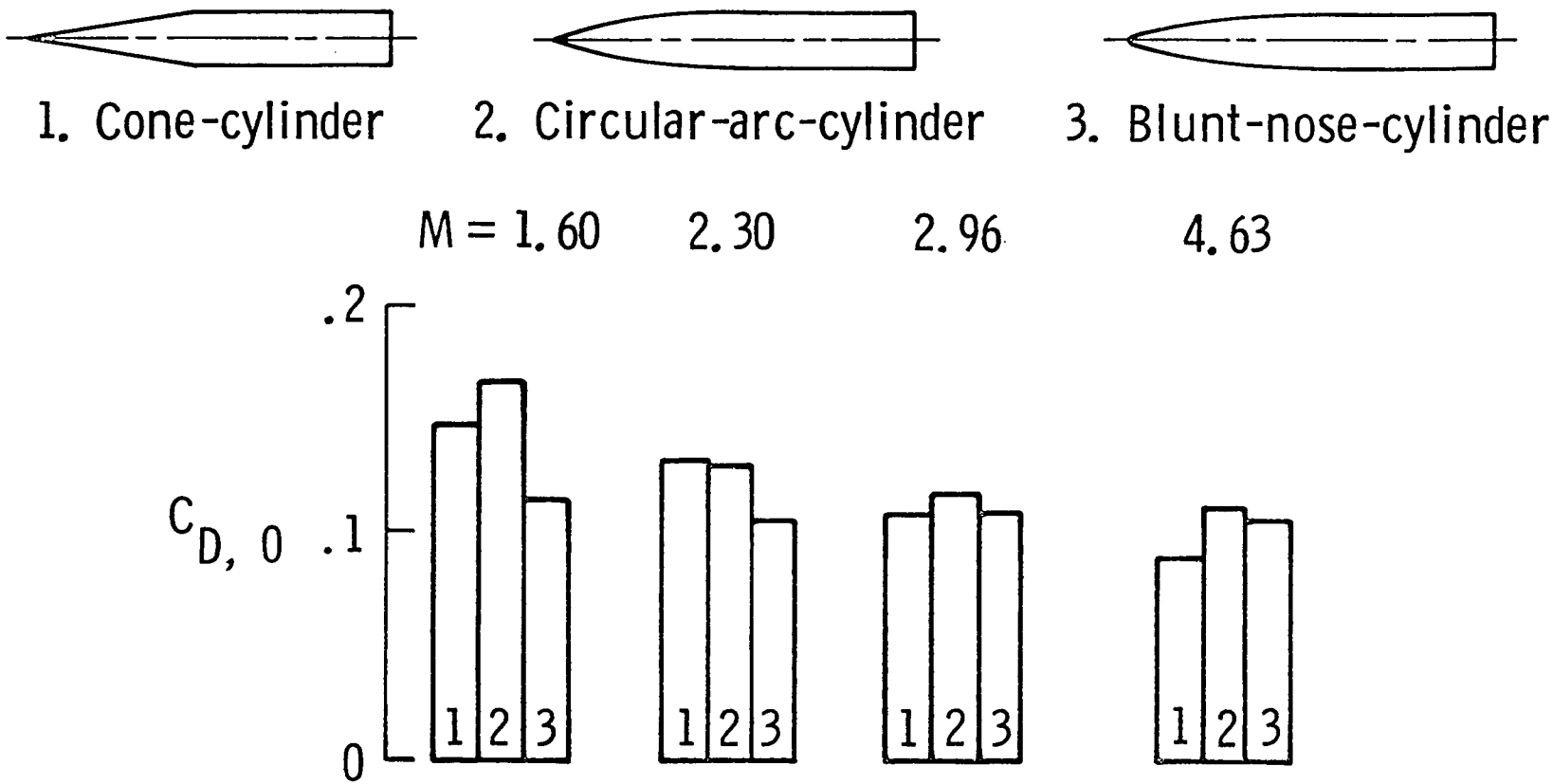

Figure 6.- Minimum drag comparison for various forebodies with cylindrical afterbody.

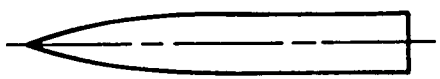

2. Circular-arc-cylinder

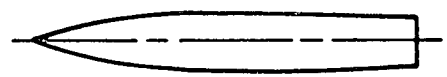

4. Circular-arc-circular-arc

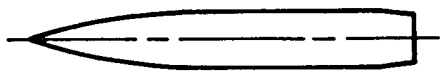

5. Circular-arc-cylinder-boattail

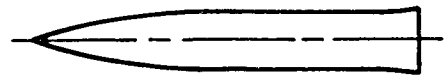

6. Circular-arc-cylinder-flare

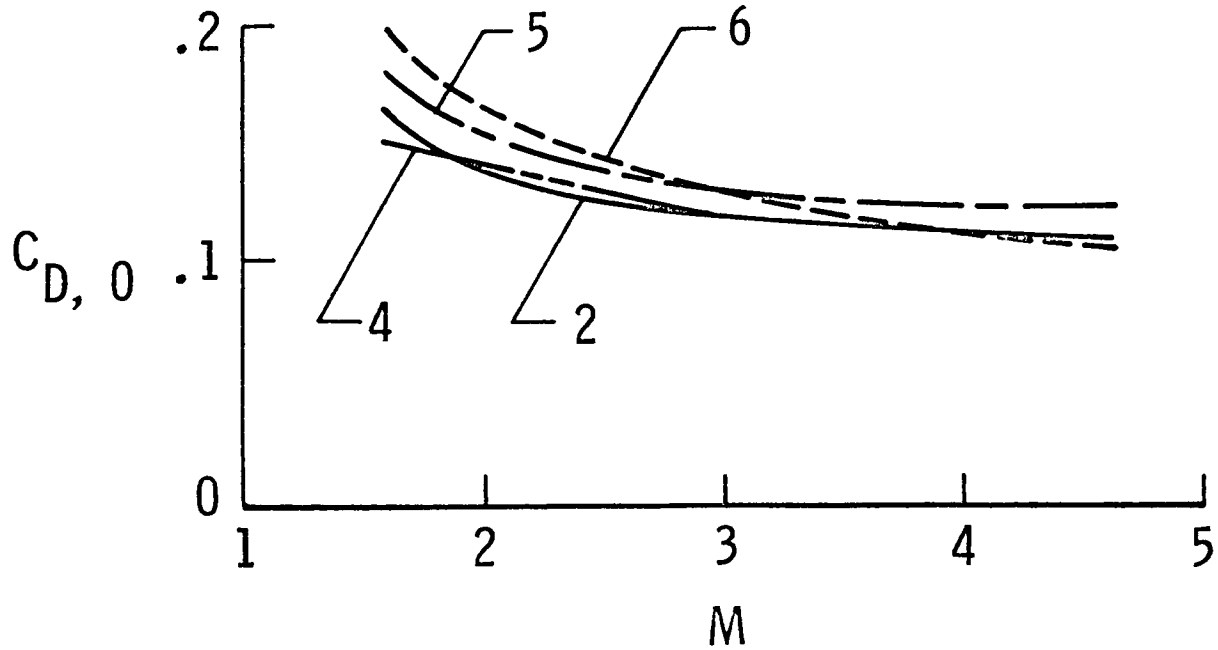

Figure 7.- Afterbody effect on minimum drag with circular arc forebody.

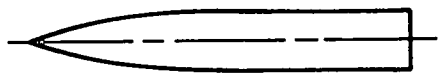

2. Circular-arc-cylinder

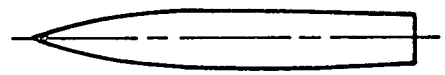

4. Circular-arc-circular-arc

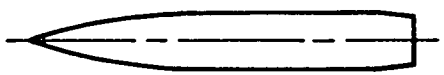

5. Circular-arc-cylinder-boattail

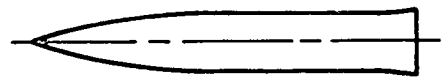

6. Circular-arc-cylinder-flare

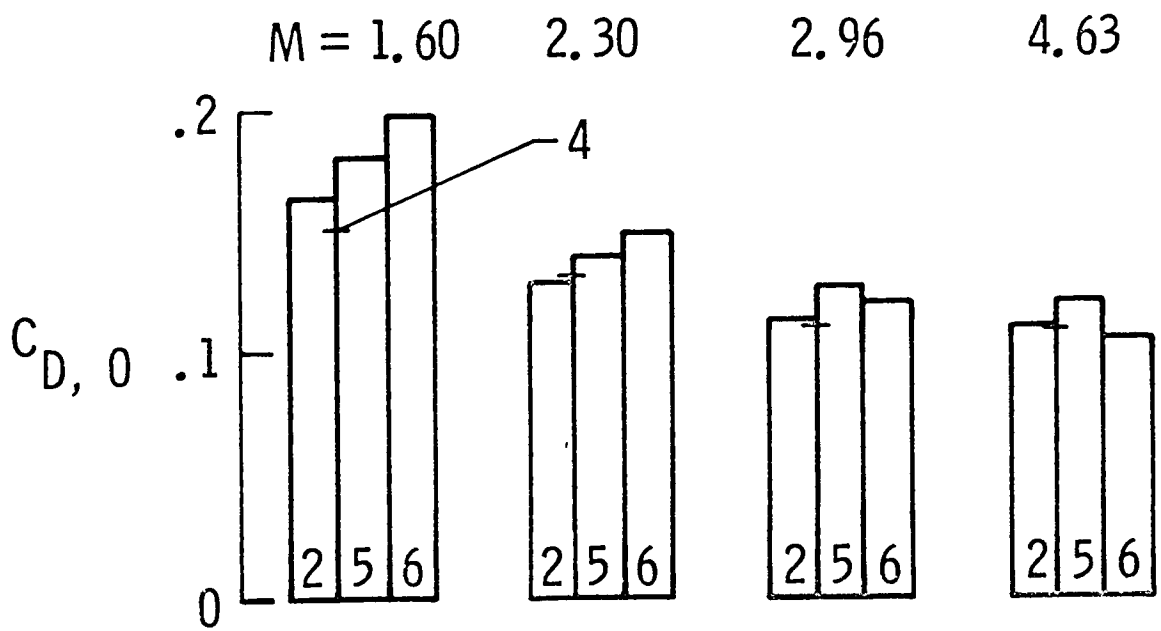

Figure 8.- Minimum drag comparison for various afterbodies with circular arc forebody.

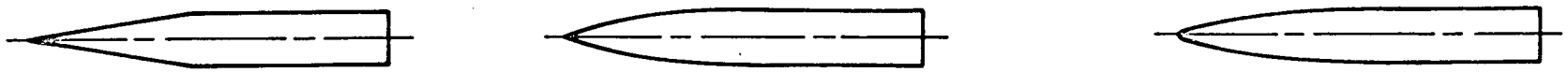

1. Cone-cylinder 2. Circular-arc-cylinder 3. Blunt-nose-cylinder

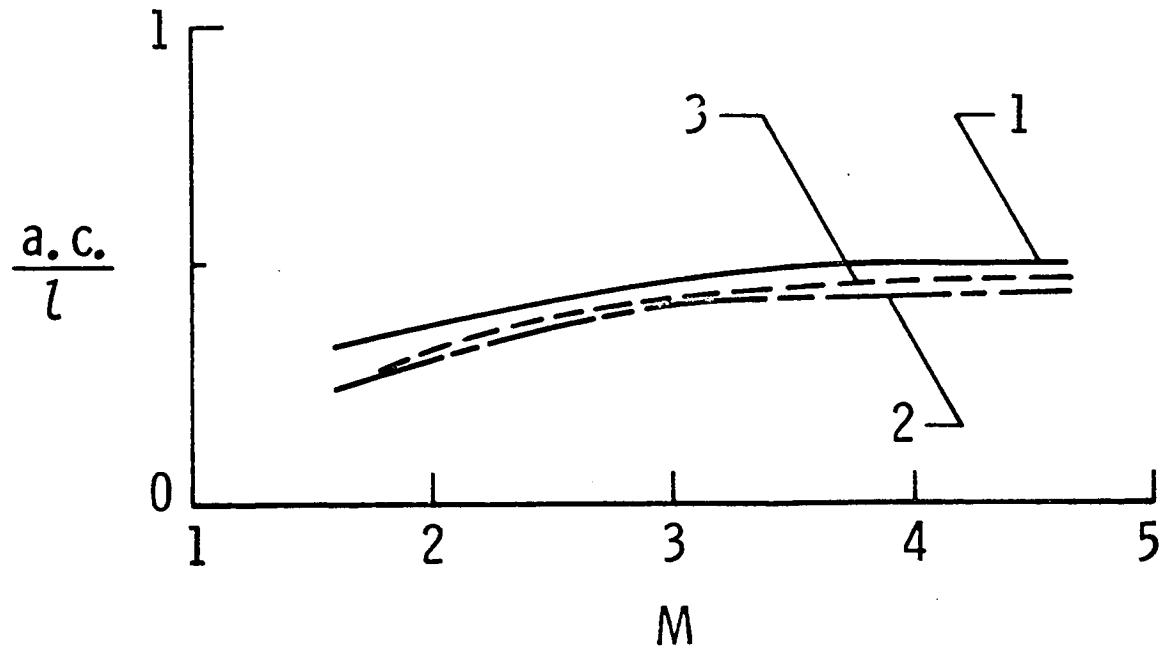

Figure 9.- Forebody effect on aerodynamic center with cylindrical afterbody.

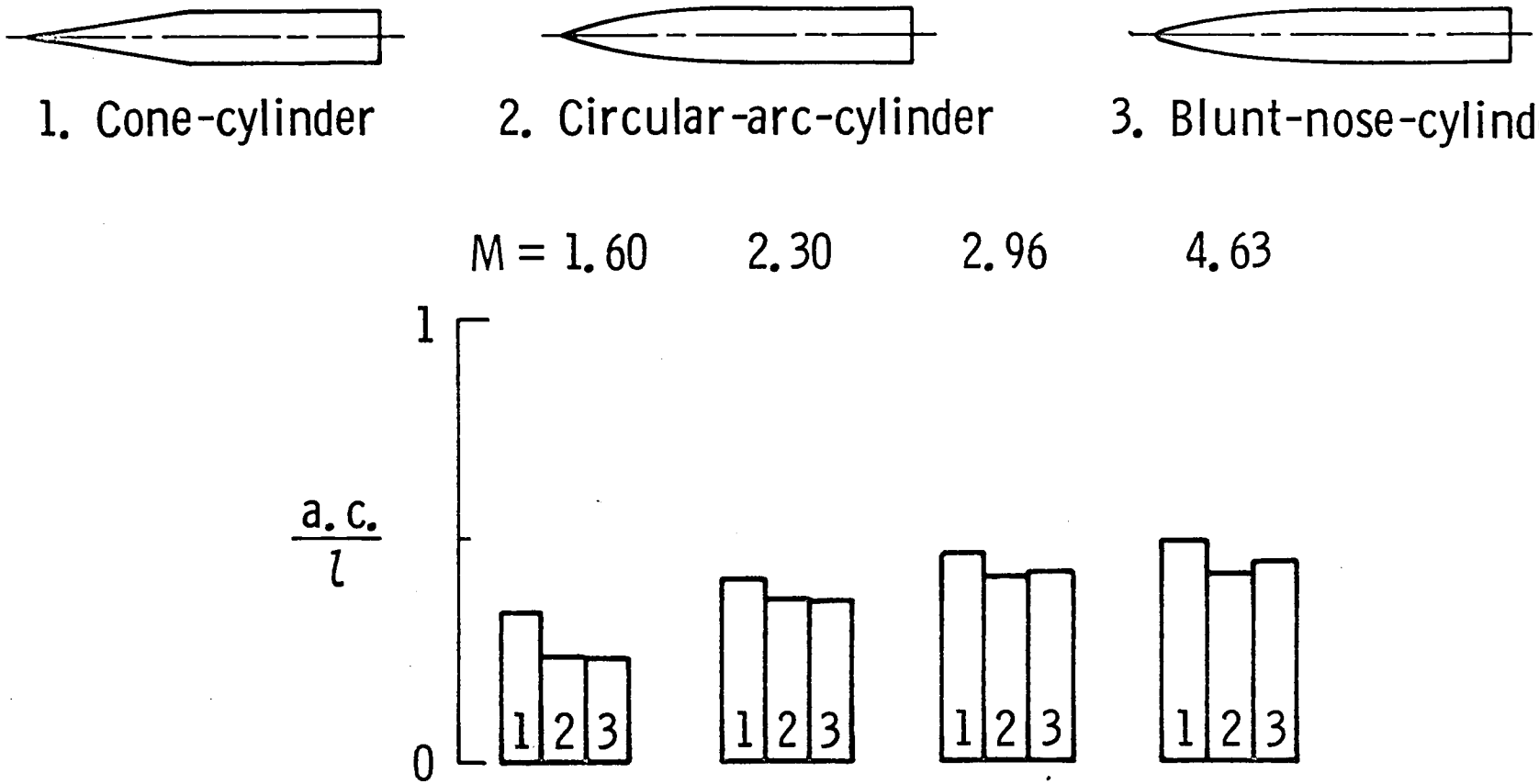

Figure 10.- Aerodynamic center comparison for various forebodies with cylindrical afterbody.

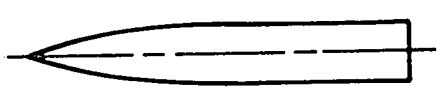

2. Circular-arc-cylinder

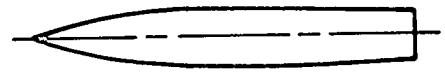

4. Circular-arc-circular-arc

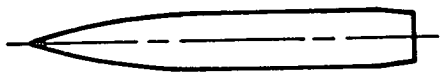

5. Circular-arc-cylinder-boattail

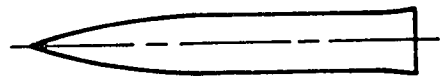

6. Circular-arc-cylinder-flare

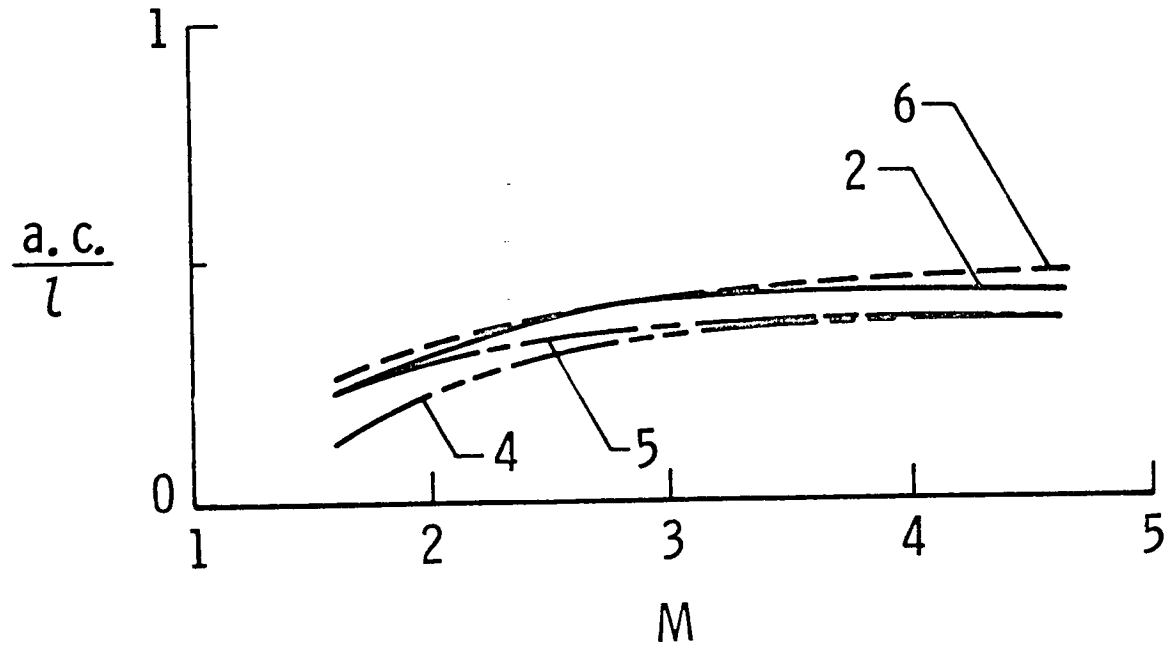

Figure 11.- Afterbody effect on aerodynamic center with circular arc forebody.

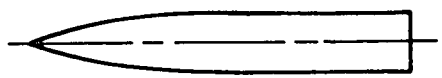

2. Circular-arc-cylinder

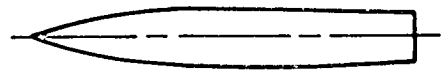

4. Circular-arc-circular-arc

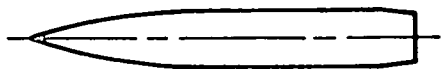

5. Circular-arc-cylinder-boattail

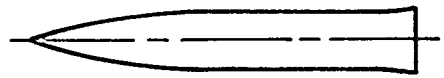

6. Circular-arc-cylinder-flare

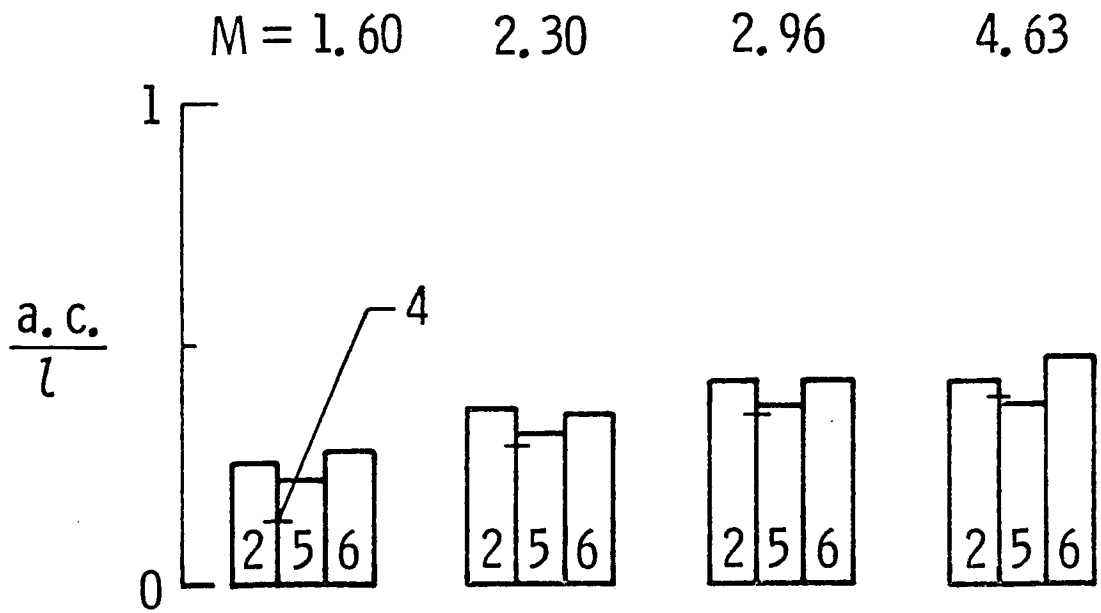

Figure 12.- Aerodynamic center comparison for various afterbodies with circular-arc forebody.

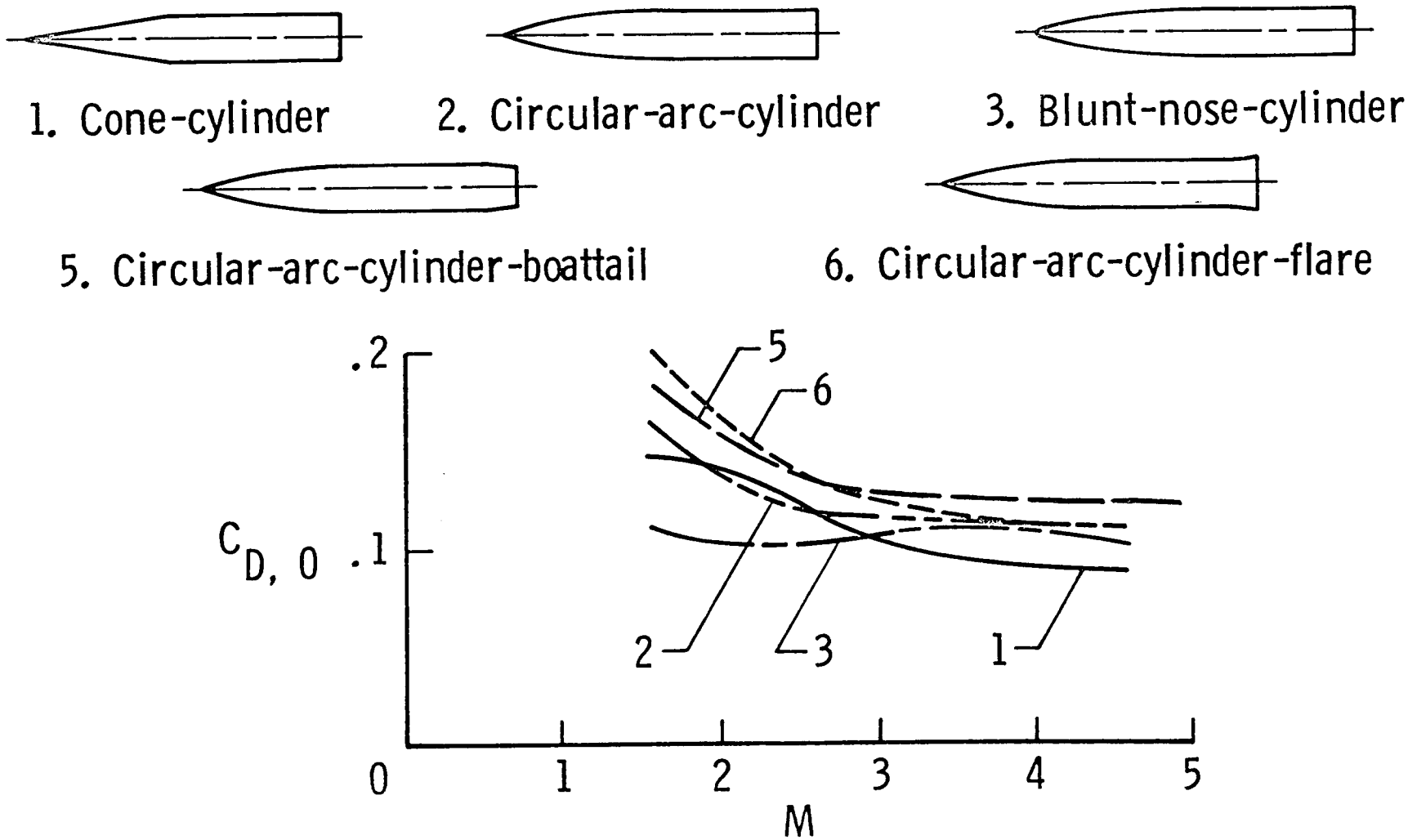

Figure 13.- Minimum drag variations for various forebodies and afterbodies.

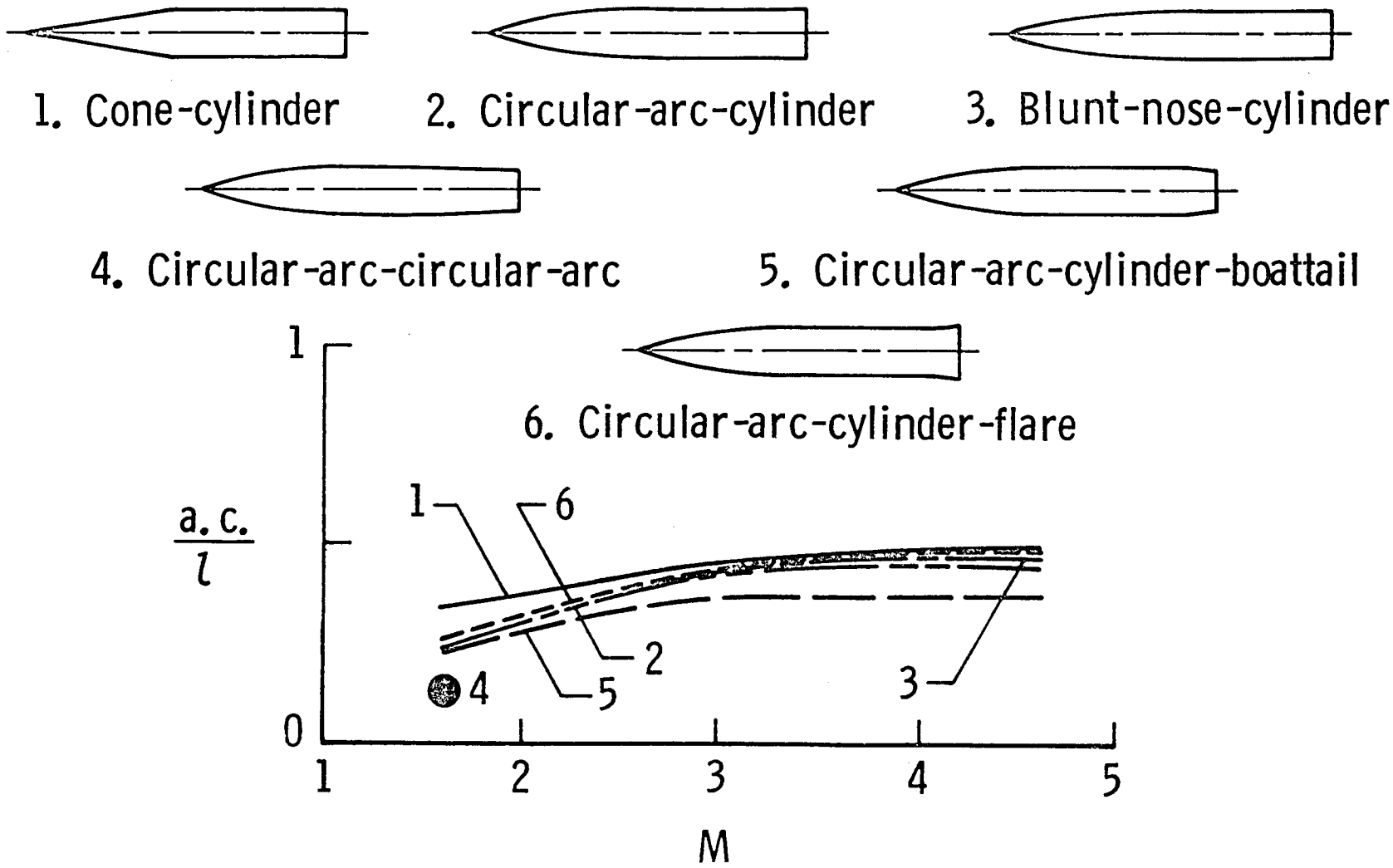

Figure 14.- Aerodynamic center variations for various forebodies and afterbodies.

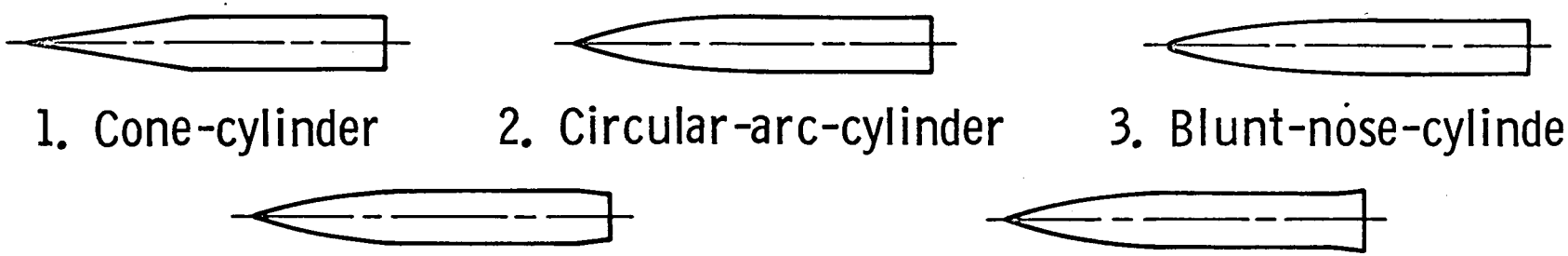

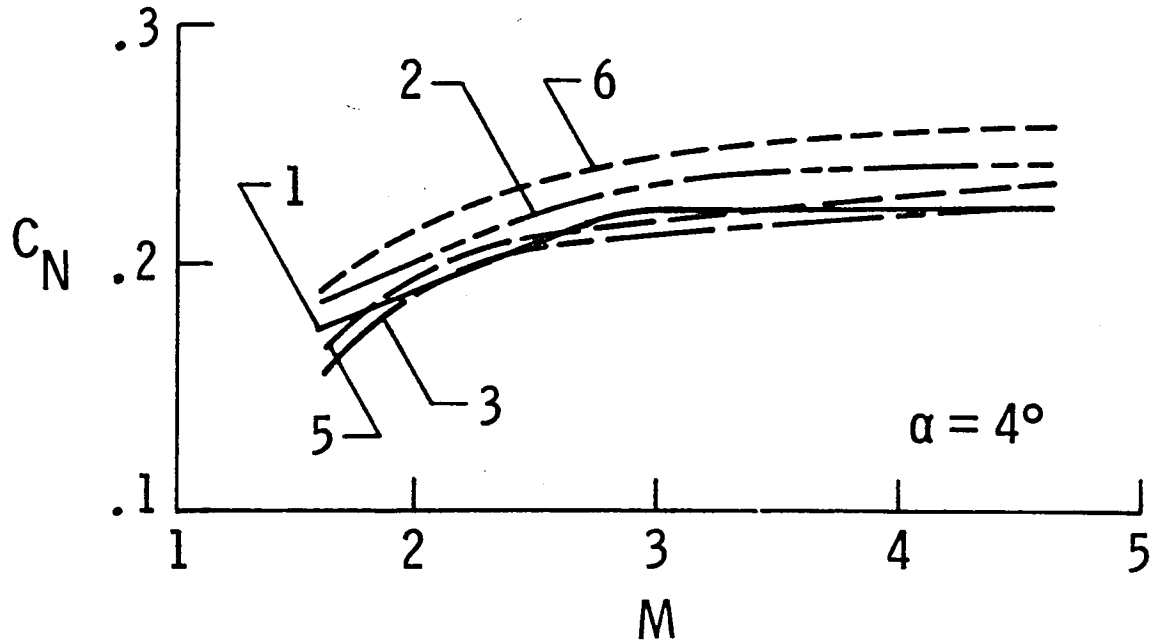

Figure 15.- Normal force variations for various forebodies and afterbodies at α = 4°.

1. Report No.	2. Government Accession No.	3. Recipient's Catalog No.
NASA TM-86345		

4. Title and Subtitle	5. Report Date
EFFECTS OF BODY SHAPE ON THE AERODYNAMICS OF A BODY OF REVOLUTION AT MACH NUMBERS FROM 1.6 TO 4.6	January 1985
	6. Performing Organization Code 505-43-43-01
7. Author(s) M. Leroy Spearman	8. Performing Organization Report No.
9. Performing Organization Name and Address NASA Langley Research Center Hampton, Virginia 23665	10. Work Unit No.
	11. Contract or Grant No.
12. Sponsoring Agency Name and Address National Aeronautics and Space Administration Washington, DC 20546	13. Type of Report and Period Covered Technical Memorandum
	14. Sponsoring Agency Code

15. Supplementary Notes

Colateral release with paper presented at the American Defense Preparedness Association 8th International Symposium on Ballistics, Orlando, FL, Oct. 1984.

16. Abstract

The aerodynamic characteristics for several bodies of revolution have been determined from wind tunnel tests at Mach numbers from 1.6 to 4.63. Six bodies, each having a length-to-diameter ratio of 6.67, were investigated. Geometric modifications included forebody shape, afterbody shape, and midsection slope. Significant aerodynamic changes were observed to be functions of geometric change and Mach number. Because of the aerodynamic dependence on geometry as well as Mach number, it is obvious that a number of trades must be considered in selecting a projectile shape.

17. Key Words (Suggested by Author(s))	18. Distribution Statement
Projectiles Bodies of revolution Aerodynamic characteristics	Unclassified - Unlimited Subject Category 01

19. Security Classif. (of this report)	20. Security Classif. (of this page)	21. No. of Pages	22. Price
Unclassified	Unclassified	22	A02

For sale by the National Technical Information Service, Springfield, Virginia 22161